constructed our stimulus signals based on different inputs to calculate the output response based on the augmented input. We measured the voltage waveforms at the output of the first-order and the second-order Gaussian derivatives pulse generators. These differentiators reduce the rise time by almost 50%, that is, half-rise time pulse shaping, and a summation is used for passing only the positive parts while removing the negative ringing portion. These differentiators network, however, also attenuates the pulse amplitude as expected. The fall time and pulse width are further reduced using the differentiators and summing the various responses using Matlab as shown in Figure 3. The rise time characteristics for the Gaussian pulse is 123 ps, for the Monocycle pulse is 92 ps, and for the Doublet pulse is 56 ps. It is found out that using one differentiator a drop of 31 ps, and using two differentiators the drop is larger and amounts to 67 ps, that is, significant rise time decrease can be achieved in the first peak of these signals [7,8]. Figure 7 shows the measured impulse TDR observed at port 1 of the defected structures, with a 50 Ω termination on port 2. The excitation sources are $M_0(t)$, $M_1(t)$, and $M_2(t)$ as shown in Figure 3. Also Figure 7 indicates a discrepancy between measured data and simulated results. This discrepancy is fabrication and assembly tolerances. The time characteristics for the measured TDR results shown in Figure 7 are summarized in Table 1.

4. CONCLUSION

A novel pulse excitation is used instead of the Gaussian pulse in TDR. The proposed modified TDR is less expensive than a vector network analyzer, very practical as it is based on more realistic signals rather than assuming ideal impulses or steps. The modified codes TDR has a wider bandwidth that leads to higher accuracy localization of the various discontinuities along a line. Higher accuracy has been achieved for higher order M signals in the range of 15 ps, which is significant in localizing discontinuities. Further effort is under way too to tighten measurements tolerances for even closer results to ground truth data.

ACKNOWLEDGMENT

The authors are thankful to Microwave Technology (MWT) Company staff for their beneficial and professional help (www.microwave-technology.com).

REFERENCES

1. R. Tamas, G. Caruntu, and D. Popa, A time-domain measuring technique for ultra-wide band antennas, Microwave Opt Technol Lett 53 (2011), 281–286.
2. Time Domain Reflectometry Theory, Agilent Technologies, Palo Alto, CA, USA, Application Note 1304-2, 2006.
3. M. Ojaroudi and E. Mehrshahi, Novel band-stop small square monopole antenna by using interdigital strip protruded inside the rectangular slot as a band-stop filter with its equivalent circuit based in TDR analysis for UWB applications, In: International Symposium on Antennas and Propagation (ISAP), Nagoya, —Japan, 2012.
4. M. Ojaroudi and E. Mehrshahi, High accuracy time domain modeling of microstrip discontinuities by using modified TDR based on barker codes with flat spectrum and integrated side-lobes, ACES J 28 (2013), 374–379.
5. G.E. Andrews, R.A. Askey, and R. Roy, Special functions, Cambridge University Press, Cambridge, UK, 2000.
6. C. Zhang and A.E. Fathy, Reconfigurable pico-pulse generator for UWB applications, In Proceedings of Microwave Symposium Digest, San Francisco, CA, June 2006, pp. 407–410.
7. C.H. Cheng, C.H. Tsai, and T.L. Wu, A novel time domain method to extract equivalent circuit model of patterned ground structures, IEEE Microwave Wireless Compon Lett 17 (2010).
8. M. Ojaroudi and E. Mehrshahi, Bandwidth enhancement of small square monopole antennas by using defected structures based on time domain reflectometry analysis, ACES J 28 (2013), 620–627.

ARRAY OF SPATIAL POWER COMBINATION FOR WIDE ANGLE SECTOR COVERAGE

Le Chang, Zhijun Zhang, Yue Li, and Zhenghe Feng
State Key Lab of Microwave and Communications, Department of Electronic Engineering, Tsinghua University, Beijing 100084, China; Corresponding author: zjzh@tsinghua.edu.cn

Received 14 April 2014

ABSTRACT: *This study investigates the feasibility of using spatial power combination in small-scale array applications that require sector coverage. A patch antenna array is used to verify the concept. The simulated result of the proposed array shows that the −6 dB angle coverage is 132° from 24° to 156° in elevation plane and the −10 dB return loss bandwidth is 4.6%. The optimized measured result indicates that the −6 dB angle coverage is 134° from 20° to 154° in elevation plane.* © 2014 Wiley Periodicals, Inc. Microwave Opt Technol Lett 56:2990–2993, 2014; View this article online at wileyonlinelibrary.com. DOI 10.1002/mop.28756

Key words: *spatial power combination; high power; patch array; wide angle coverage; flat response*

1. INTRODUCTION

Spatial power combination has been widely used in many microwave and millimeter-wave systems in recent years. In a communication system, the improvement of the system transmission power means better communication quality, stronger anti-interference ability, and a longer range of communication distance. As the operating frequency of semiconductor solid-state devices increases into the millimeter-wave band, the size of the devices is reduced, thus resulting in a decrease in their power-handling capability [1]. Therefore, the power combination technique is important in increasing system transmission power and thus has become a hot area in wireless communications today.

The power combination technique can be classified into two types: circuit power combination and spatial power combination. The circuit-based power combination approach has limits in device power density and combining efficiency because with the increase in the number of active components, the losses induced by a combination circuit increase accordingly, which leads to a reduction in the overall combining efficiency.

In comparison, spatial power combination has the advantage of high combination efficiency, and this efficiency is hardly affected by the number of components. Many researches on spatial power combination have been published. In [2], a high-power microwave based on spatial power combination is presented. Several high-power microwave sources are used to launch microwaves with the same frequency and a set of specific phases to form a high-power electromagnetic beam in a specific direction and over a specific distance. In [3], a system of 60-GHz tray amplifiers is proposed. A 17-element dipole array is fed by a waveguide horn, and then each dipole transfers energy to a tray containing 16 MMIC output amplifiers; the output signal from the 17, 16 ports is collected by a horn with

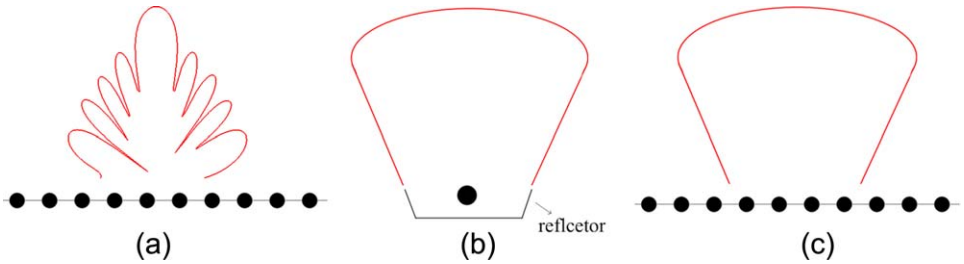

Figure 1 (a) Traditional antenna array with equal amplitude and equal phase, (b) a single antenna with a backed reflector, and (c) antenna array with sector coverage. [Color figure can be viewed in the online issue, which is available at wileyonlinelibrary.com]

focusing lenses. This system generates 35-W output power at 61 GHz with a high gain value of 60 dB. The achievement of high power through spatial power combination is reported elsewhere in the literature [4–6]. The main goal of the existing researches is to obtain the highest effective isotropic radiated power. This means that all the elements of the antenna array are excited in phase; thus, these arrays not only obtain high output power but also have a high array gain in a specific direction, resulting in directional beams with narrow angle coverage.

In cellular communication, sector antennas are widely adopted because they can cover a large service area without requiring alignment between the receiving and transmitting antennas [7]. They are also widely used in tracking and surveillance, satellite on-the-move communications, and the shore early-warning radar systems [8]. Antennas with shaped beams are able to achieve sector coverage. The design of the synthesizing shaped-beam problem has attracted much attention in the past decades. Array antennas are used frequently to obtain the desired radiation patterns by optimizing the phase and amplitude distribution of the array elements [9]. The cosecant beam, flat-top beam, and pencil beam are three types of patterns commonly used in beam shaping [10,11]. The existing researches on beam forming normally adopt large-scale arrays. For power combination applications, a smaller-scale array is more feasible. To simplify the power amplifier design, all amplifiers should have the same output power, which means only phases can be optimized.

In this letter, we investigated wide angle sector coverage of the elevation pattern using the spatial power combination technique. A patch array is used as an example to verify the concept. As mentioned above, due to the limitation in the power-carrying capability of the microwave sources and the front end of the radio-frequency circuit, each element of the proposed array can deliver only limited power. High power can be obtained by spatial power combination: by combining the low power elements of the antenna array to achieve high power, all the elements of the antenna array work in a state of saturated input power. The degree of design freedom is only the phase distribution, whereas the amplitudes of the excitation maintain the same maximal sustainable power. A set of optimized phases is fed to the array elements to achieve a flat response in elevation plane. The simulated and modified measured results show that the patch array is able to achieve sector coverage in elevation plane.

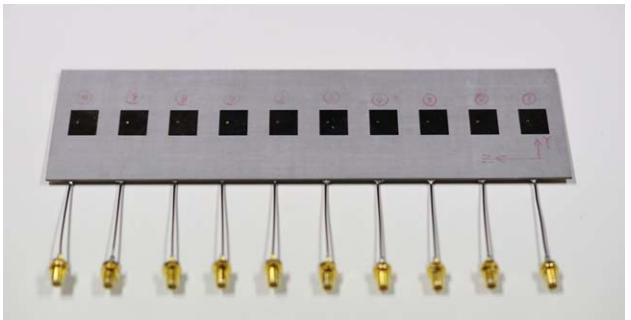

Figure 2 Photograph of the fabricated prototype. [Color figure can be viewed in the online issue, which is available at wileyonlinelibrary.com]

2. POWER COMBINATION FOR WIDE ANGLE SECTOR COVERAGE

Basically, traditional equal amplitude and equal phase antenna arrays are aimed at obtaining a high directivity beam, as shown in Figure 1(a). In contrast, sector antennas are aimed at achieving wide angle sector coverage. A single antenna backed with a reflector, as shown in Figure 1(b), can achieve such radiation characteristic, but it cannot deliver high power. Thanks to the concept of spatial power combination, we can achieve wide angle sector coverage with high power in space using an antenna array, as depicted in Figure 1(c).

Without loss of generality, a patch array, as shown in Figure 2, is used in verification. The proposed array is printed on top of a substrate with dimensions of 264 and 80 mm. The substrate has a thickness of 1.6 mm, permittivity of 2.55, and tangential loss of 0.002. The element is a rectangular patch with dimensions of 14.55 and 18.46 mm and a center frequency of 5.9 GHz. The interelement spacing of the proposed array is half of the wavelength in free space. Ten 50-Ω semirigid cables are used to feed the array. These elements are excited with the same power but at different phases. The phase distribution shown in Table 1 was acquired through a stochastic optimization algorithm with the use of the Matlab software. As a result, the amount of radiation power in space is 10 times that of a single element. The simulated elevation radiation pattern of the proposed array is described in Figure 3, which shows that the −6 dB gain fluctuation angle is 132° from 24° to 156° and the −3 dB gain fluctuation angle is 56° from 56° to 122°. Thus, sector coverage and high power are obtained simultaneously in the simulation. The simulated result is obtained with the high frequency structure simulator full-wave simulation software.

3. RESULTS AND DISCUSSION

The measured *s*-parameters and the radiation patterns are obtained from a vector network analyzer and an anechoic chamber, respectively.

TABLE 1 Phases Values for Simulation (Unit: Degree)

−106	49	−182	−44	0	0	−44	−182	49	−106

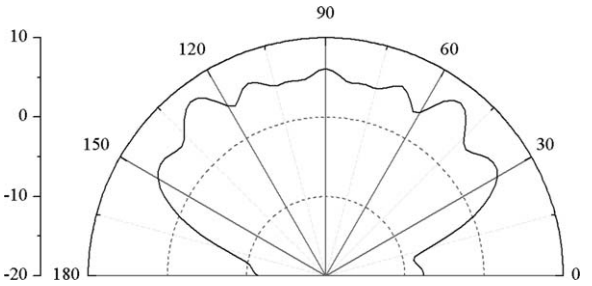

Figure 3 Simulated radiation pattern in elevation plane with an optimized phase distribution

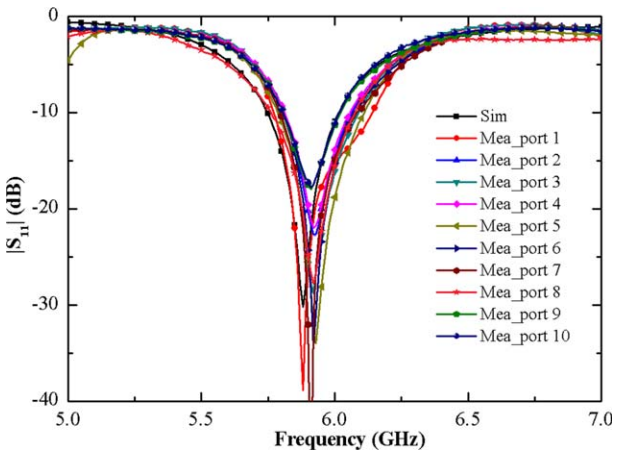

Figure 4 Simulated and measured return loss of the proposed array. [Color figure can be viewed in the online issue, which is available at wileyonlinelibrary.com]

Figure 4 shows the simulated and measured reflection coefficients of the proposed array. The simulated reflection coefficient, shown as a black line with a square symbol, has a −10 dB impedance bandwidth of 270 MHz (5.75–6.02 GHz) centered at 5.9 GHz. The curve Mea_port i ($i = 1$–10) represents the active reflection coefficient of the port i when the patch i is excited and others are connected to a matched load. The 10

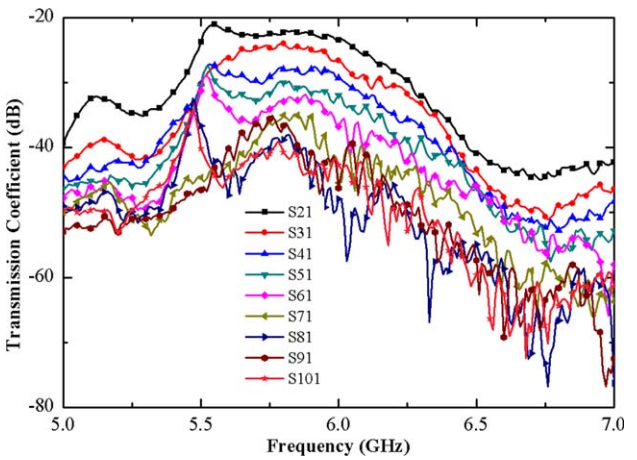

Figure 5 Measured magnitude of transmission coefficient. [Color figure can be viewed in the online issue, which is available at wileyonlinelibrary.com]

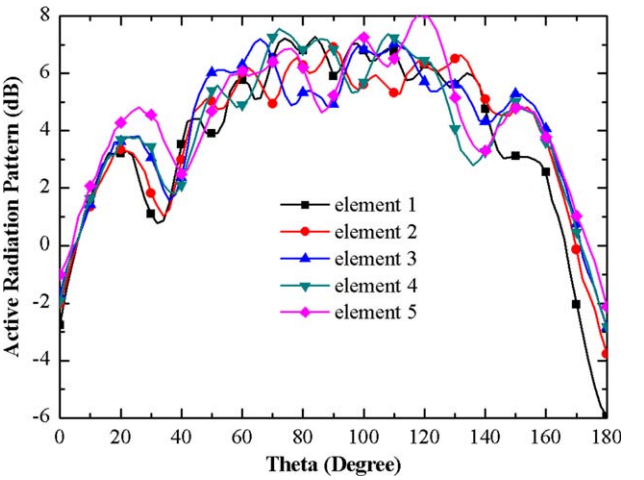

Figure 6 Active radiation pattern of five elements. [Color figure can be viewed in the online issue, which is available at wileyonlinelibrary.com]

curves almost overlap with the simulated curve, and their resonant frequencies are clustered at 5.9 GHz, with an impedance bandwidth range of 210–370 MHz.

We also investigated the mutual coupling effect of the elements. Figure 5 describes the magnitude of the transmission coefficients from port i ($i = 2$–10) to port 1 when the rest ports are connected to a matched load. The data show that all the transmission coefficients are better than −20 dB; thus, the coupling between arbitrary two ports can be neglected.

Figure 6 depicts the active radiation patterns of the half array elements in the *XZ*-plane. When one of the elements is excited, the rest are connected to a matched load. As shown in the figure, the five patterns are different from each other. This phenomenon is due to the different relative positions between the driven element and the rest of the elements, which indicates that the elements do not operate independently but instead influence each other.

As presented in Figure 7, the measured elevation radiation pattern, shown as a line with a round symbol, deviates considerably from the simulated one and has obvious fluctuations. The deviation is attributed to the accumulation effect of the unequal length of the cables and other uncertainty factors, such as fabrication errors and measurement errors. The fluctuations are due to the fact that the optimized phases are not optimal for the measured data. To verify the feasibility of the concept in practical application, the same stochastic optimization algorithm is applied to dispose of the measured data and acquire another set

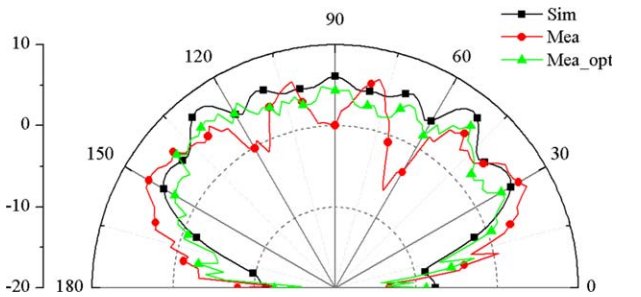

Figure 7 Simulated, measured, and optimized measured radiation pattern in elevation plane. [Color figure can be viewed in the online issue, which is available at wileyonlinelibrary.com]

TABLE 2 Phases Values for Measurement (Unit: Degree)

101	−68	−196	−22	0	0	−22	−196	−68	101

of optimized phase distributions, as shown in Table 2. The corresponding elevation radiation pattern is depicted as a line with a triangular symbol. The −6 dB gain fluctuation angle is 134° from 20° to 154°, and the −3 dB gain fluctuation angle is 52° from 54° to 116°. Therefore, the feasibility of using spatial power combination in applications that require sector coverage is verified.

We can expand the elements of the array by following this principle to get a much higher power level. We can also use other types of array elements, such as dipole, loop, and slot, among others.

4. CONCLUSION

In this letter, the feasibility of using spatial power combination for wide angle sector coverage of the elevation pattern is investigated, and a patch array is used to verify the concept. Considering the power-carrying capability of radio-frequency devices, high radiation power can be obtained by a combination of multiple low-power antenna elements. Then an optimized phase distribution is fed to the array elements to achieve a flat response in a wide angle. The simulated and modified measured results show that the proposed array is capable of achieving sector coverage in elevation plane and high power simultaneously.

ACKNOWLEDGMENT

This work is supported by the National Basic Research Program of China under Contract 2013CB329002.

REFERENCES

1. M. P. DeLisio and R. A. York, Quasi-optical and spatial power combining, IEEE Trans Microwave Theory Tech 50 (2002), 929–936.
2. J. Benford, J. A. Swegle, and E. Schamiloglu. High power microwaves, 2nd ed., New York, CRC press, 2007.
3. J. J. Sowers, D. J. Pritchard, A. E. White, W. Kong, O. S. A. Tang, D. R. Tanner, and K. Jablinskey, A 36 W, V-band, solid-state source, In: Microwave Symposium Digest, 1999 IEEE MTT-S International, Anaheim, CA, USA, June 13–19, 1999, pp. 235–238.
4. B. Deckman, D. S. Deakin, Jr., E. Sovero, and D. Rutledge, A 5-watt, 37-GHz monolithic grid amplifier, In: Microwave Symposium Digest, 2000 IEEE MTT-S International, Boston, MA, USA, June 11–16, 2000, pp. 805–808.
5. N.-S. Cheng, P. Jia, D. B. Rensch, and R. A. York, A 120-W X-band spatially combined solid-state amplifier, IEEE Trans Microwave Theory Tech 47 (1999), 2557–2561.
6. S. Ortiz, J. Hubert, L. Mirth, and A. Mortazawi, A 25 W Ka-band quasi-optical amplifier array, IEEE Trans Microwave Theory Tech, in press.
7. C. Deng, P. Li, and W. Cao, A high-isolation dual-Polarization patch antenna with omnidirectional radiation patterns, IEEE Antennas Wireless Propag Lett 11 (2012), 1273–1276.
8. I. Khalifa and R. Vaughan, Optimal configuration of multi-faceted phased arrays for wide angle coverage, In: Vehicular Technology Conference, Dublin, Ireland, April, 2007, pp. 304–308.
9. M. Karimipour, A. Pirhadi, and N. Ebrahimi, Accurate method for synthesis of shaped-beam non-uniform reflectarray antenna, IET Microwaves Antennas Propag 11 (2013), 1247–1253.
10. T. Isernia, A. Massa, A. F. Morabito, and P. Rocca, On the optimal synthesis of phase-only reconfigurable antenna arrays, In: Proceedings of the 5th European Conference on Antennas and Propagation (EUCAP), Rome, April, 2011, pp. 2074–2077.
11. A. Akdagli, K. Guney, and D. Karaboga, Touring ant colony optimization algorithm for shaped beam pattern synthesis of linear antenna, Electromagnetics 26 (2006), 615–628.

HIGH SELECTIVITY AND CM SUPPRESSION WIDEBAND BALANCED BPF

Hong-Wei Deng, Yong-Jiu Zhao, Ying He, Hao Liu, and Hong-Li Wang

The Key Laboratory of Radar Imaging and Microwave Photonics (Nanjing Univ. Aeronaut. Astronaut.), Ministry of Education, College of Electronic and Information Engineering, Nanjing University of Aeronautics and Astronautics, Nanjing, 210016, China; Corresponding author: hwdeng@nuaa.edu.cn

Received 23 April 2014

ABSTRACT: *In this letter, a novel wideband balanced bandpass filter (BPF) with high selectivity and common-mode (CM) suppression is constructed with slotline resonator. When the intersection points of the microstrip feedline and slotline resonator are close to the midpoint of the slotline resonator, the coupling between the second mode and microstrip feedline can be suppressed. Making use of this feature, the wideband single-ended filter with wide upper-stopband performance is designed using the slotline resonators and two quarter-wavelength microstrip resonators paralleled to the slotline resonator with tapped-line coupling at their short-circuited ends. Further, high-selectivity fifth-order wideband single-ended filter and corresponding balanced BPF are designed with parallel coupling structures between two slotline resonators. The fifth-order wideband balanced filter is designed and fabricated, and good agreement between measurements and simulations is obtained. The measured CM suppressions are better than 54 dB within the whole differential-mode passband.* © 2014 Wiley Periodicals, Inc. Microwave Opt Technol Lett 56:2998–3003, 2014; View this article online at wileyonlinelibrary.com. DOI 10.1002/mop.28755

Key words: *balanced filter; high common-mode suppression; high selectivity; slotline resonator; wideband*

1. INTRODUCTION

Balanced filters are essential in communication systems due to their crucial role in reducing the interference, noise, and crosstalk between different elements of the system [1–5]. The destination of the balanced filter is to make the differential mode to have high selectivity for the desired frequency response, while the common mode should be suppressed over a wider frequency band. Recently, the wide and ultrawideband (UWB) systems attract much attention to satisfy the requirement of high data rate transmission. Numerous interests have been aroused from both academic and industrial areas toward differential wideband technology.

The wideband single-ended filter with slotline resonator was analyzed in [6] with compact size and good electrical performance. In 2007, a compact filter with a faction bandwidth (FBW) of 60% [7] was presented using a slotline resonator and two quarter-wavelength microstrip resonator (QWRs). In the same year, two wideband filters using the triple-mode slotline resonator and the microstrip-slotline transition were designed with a FBW up to 120% [8,9]. Further, the modified triple-mode UWB slotline filters in [10,11] were designed to obtain good differential-mode (DM) response. Ultrawide passband in [8–11]